

Looking at Blazar Light Curve Periodicities with Gaussian Processes

STEFANO COVINO,¹ MARCO LANDONI,¹ ANGELA SANDRINELLI,¹ AND ALDO TREVES^{1,2}

¹*INAF / Brera Astronomical Observatory, via Bianchi 46, 23807, Merate (LC), Italy*

²*Università degli Studi dell'Insubria, Via Valleggio 11, 22100 Como, Italy*

Submitted to AJ

ABSTRACT

Temporal analysis of blazar flux is a powerful tool to draw inferences about the emission processes and physics of these sources. In the most general case, the available light curves are irregularly sampled and influenced by gaps, and in addition are also affected by correlated noise, making their analysis complicated. Gaussian processes may offer a viable tool to assess the statistical significance of proposed periods in light curves characterized by any sampling and noise pattern. We infer the significance of the periods proposed in the literature for two well known blazars with multiple claims of possible year-long periodicity: PG 1553+113 and PKS 2155-304, in the high-energy and optical bands. Adding a periodic component to the modeling gives a better statistical description of the analyzed light curves. The improvement is rather solid for PG 1553+113, both at high energies and in the optical, while for PKS 2155-304 at high energies the improvement is not yet strong enough to allow cogent claims, and no evidence for periodicity emerged by the analysis in the optical. Modeling a light curve by means of Gaussian processes, in spite of being relatively computationally demanding, allows us to derive a wealth of information about the data under study and suggests an original analysis framework for light curves of astrophysical interest.

Keywords: (Galaxies:) BL Lacertae objects: general – (Galaxies:) BL Lacertae objects: PG 1553+113 – (Galaxies:) BL Lacertae objects: PKS 2155-304 – Methods: statistical

1. INTRODUCTION

Blazars (e.g., Urry 2012) are one of the most frequent targets for monitoring programs at essentially any wavelength because of their variability, from the radio band to the highest energies. A natural outcome of this intense monitoring is the availability of long time series that offer a treasure of possible information about this class of sources (e.g., Ryan et al. 2019). One of the most interesting topics that can be addressed with well sampled time series is the identification of possible periodic or quasi-periodic behaviors. Several authors have indeed proposed quasi-periodic oscillations (QPO) for blazars at various levels of statistical significance (e.g., Lehto & Valtonen 1996; Zhang et al. 2014; Sandrinelli et al. 2014; Ackermann et al. 2015; Cutini et al. 2016; Sandrinelli et al. 2016a,b; Stamerra et al. 2016; Sandrinelli

et al. 2017; Covino et al. 2017; Cavaliere et al. 2017; Prokhorov & Moraghan 2017; Zhang et al. 2017a,b,c; Tavani et al. 2018; Sandrinelli et al. 2018; Bhatta 2019; Covino et al. 2019; Rieger 2019; Chevalier et al. 2019; Ait Benkhali et al. 2019; Bhatta & Dhital 2019).

This interest is not misplaced, since QPOs in blazars could be powerful diagnostics of different phenomena associated to blazar phenomenologies (e.g., Lindfors et al. 2016). Interpretation of possible QPOs in blazars has recently attracted the attention of several works (e.g., Cavaliere et al. 2017; Sobacchi et al. 2017; Caproni et al. 2017; Holgado et al. 2018; Cavaliere et al. 2019; Lico et al. 2020), mainly motivated by the various claims for periodicities proposed in the last few years. One picture of interest envisages the QPOs as due to a supermassive binary black-hole systems. This might directly introduce periodicities in the observed emissions (e.g., Lehto & Valtonen 1996; Sandrinelli et al. 2014; Graham et al. 2015) or indirectly through precession of the whole system (Doğan et al. 2015). On the other hand, QPOs,

possibly of transient nature, could also be generated by instabilities in the relativistic jets or in the accretion disks (Camenzind & Krockenberger 1992; Marscher 2014; Raiteri et al. 2017).

2. TIME SERIES ANALYSIS

The analysis of time series is a fundamental tool in modern astrophysics (e.g., Vaughan 2013). Given the large variety of astronomical data we can deal with, it is natural that many different techniques can be applied. Without any claim of completeness, two general scenarios can be depicted: those to treat evenly spaced data and those to cope with the irregular sampling as is the case with astronomical observations. Evenly sampled data offer the remarkable advantage to allow analyses based on a well developed set of procedures and theorems to interpret their results (e.g., van der Klis 1989, for a comprehensive review). The case of irregularly sampled data can be dealt with the recipes developed by Lomb (1976) and Scargle (1982). The Lomb-Scargle (LS) periodogram offers a rigorous solution to the problem of detecting periodic signals in noisy time series (Bretthorst 2003; VanderPlas 2018). However, it is also known to produce distorted versions of the true periodogram and alternative approaches have also been proposed (e.g., Vio & Andreani 2018). Moreover, decomposing a light curve into harmonic series unavoidably implies a particular sensitivity to quasi-sinusoidal variations. In order to cope with periodicities with any functional form, non-parametric analysis tools have been developed (e.g., Stellingwerf 1978; Schwarzenberg-Czerny 1997; Huijse et al. 2018).

Independently of the particular analysis recipe, the problem of assessing the significance of any possible periodicity in a light curve requires one to evaluate the probability that at the frequency of interest the measured power (or any other adopted periodicity indicator) is not due, to a given confidence level, to random fluctuations. This assessment depends critically on the noise affecting the data. In case we can assume the noise is “white”, i.e. independent of the frequency, it is possible to compute exactly the significance level of any observed power. The most general case, red or correlated noise (Press 1978; Milotti 2002, 2007), is considerable more difficult and still an open problem. For evenly spaced data several approaches have been suggested (e.g., Vaughan 2010; Barret & Vaughan 2012; Guidorzi et al. 2016; Vaughan et al. 2016), while for the more common unequally spaced observations only indirect procedures can be applied. There are anyway several problems to deal with. Again, with no claim of completeness for this widely debated topic, we can men-

tion the unknown distribution of periodogram peaks, the poor measurement of population variance (Koen 1990) and the independence of the powers for a periodogram at the various frequencies. This is guaranteed only when data are evenly spaced and the periodogram is computed at the Fourier frequencies, or on any other ortho-normal frequency grid. Under this condition, a formal fit of the noise functional form is possible and inferences can be derived once the noise has been properly modeled. Otherwise, a procedure often followed consists in generating a large number of dense, long, and highly sampled simulated light-curves given a set of possible noise models (or noise model parameters, Uttley et al. 2002). Then, light-curves with the same sampling of the observed curve are obtained and statistics about the power of the derived periodograms are obtained (e.g., Ackermann et al. 2015; Bhatta 2019; Graham et al. 2015; Tavani et al. 2018; Nilsson et al. 2018). Other approaches are of course possible, depending on the specific data set in analysis. As a matter of fact, the fundamental problem of assessing the significance of peaks in astronomical periodograms have understandably always received great attention in literature (e.g. Baluev 2008; Süveges et al. 2015; Hara et al. 2017; Sulis et al. 2017).

An alternative procedure is to derive information about possible periodic behaviors working in the time rather than frequency domain (e.g., Li & Wang 2018; Feigelson et al. 2018). While often computationally expensive, working in the time domain presents several advantages. First of all, one can apply inferences with data with uncertainties normally distributed. This is not (in general) the case in the frequency domain (Israel & Stella 1996). In addition phenomena affecting analysis in the frequency domain as leakage, aliasing, etc. are unimportant or much easier to deal with. The inferences are also often made less ambiguous since one does not have to rely on asymptotic behaviors, statistical tests strictly holding only for infinite time-series, or hypotheses of stationarity (Kwiatkowski et al. 1992).

An effective approach to time series modeling in the time domain has been developed to check if the observed data can be generated by autoregressive processes (Koen 2005; Kelly et al. 2009, 2014; Lenoir & Crucifix 2018; Takata et al. 2018; Kovačević et al. 2019; Feigelson et al. 2018; Elorrieta et al. 2019). It is indeed well known that if the noise is correlated then spurious and transients quasi-periodicities can be observed (e.g., Vaughan et al. 2016). A partly different procedure, that is becoming increasingly popular in the astronomical literature (e.g., Brewer & Stello 2009; Wang et al. 2012; Haywood et al. 2014; Ivezić et al. 2014; Vanderburg et al. 2015; Rajpaul et al. 2015; Luger et al. 2016; Karamanavis

2017; Foreman-Mackey et al. 2017; Kovačević et al. 2019; Wilkins 2019; Pereira et al. 2019; Jesus et al. 2019; Chua et al. 2019) and more generally in Bayesian signal estimation, is time series analysis based on Gaussian Processes (GP, Rasmussen & Williams 2006; Roberts et al. 2012; Durrande et al. 2016; Tobar et al. 2015; Littlefair et al. 2017; Tobar 2018; Angus et al. 2018). GP analysis is intrinsically a Bayesian technique, i.e. prior information that encapsulates our assumptions on the analyzed time series (such as smoothness, stationarity or periodicity) is adopted. Then, this is updated with the information provided by the observed data via a given likelihood function. And finally, a posterior distribution of the derived parameters can be used for any inference. GP are a generalization of multivariate Gaussian distributions of variables and offer a very flexible framework for modelling unknown functions by non-parametric models. A key component of the analysis is the kernel or covariance function. Given any arbitrary pair of observations, the kernel defines the degree of similarity between the observed values. There can be a plethora of possible kernel functions (squared-exponential, Matérn, etc.), although in practice, in most cases, just a few basic functions are used (Rasmussen & Williams 2006). Kernel functions drive the degree of smoothness of the observed light-curves, and can also identify periodic behaviors and define an important connection between autoregressive time series methods and GP analysis (Rasmussen & Williams 2006; Durrande et al. 2016; Foreman-Mackey et al. 2017).

3. METHODS

Our goal is to quantify the significance of possible periodicities in blazar light-curves applying a procedure that allows us to draw inferences essentially independently of the sampling scheme of the analyzed (possibly multi-dimensional) data.

The choice of a specific covariance function can be often relatively arbitrary. A frequent choice, as in Angus et al. (2018), is the Square Exponential (SE) covariance function (Rasmussen & Williams 2006):

$$k_r = A \exp\left(-\frac{r^2}{2L^2}\right), \quad (1)$$

where $A > 0$ is the amplitude, L is the length scale of the exponential decay, and $r = (t_i - t_j)$ is the time separation between data points. This is a stationary kernel since it depends only on the data separation. The choice of the SE kernel is mainly driven by its simplicity, depending only on two parameters, A and L , although there are alternatives with the same number of parameters. In general, if L is large, the correlation between two data points largely separated will be stronger.

The SE kernel could be seen as a special case of the more general Matérn covariance function family (Rasmussen & Williams 2006; Durrande et al. 2016; Foreman-Mackey et al. 2017). The Matérn kernel functions are characterized by a parameter, ν , that drives the degree of “smoothness” of the kernel. Functions with $\nu = p - 1/2$ are the discrete time equivalent to AR (autoregressive) processes of order p . For $\nu \rightarrow +\infty$ the kernel becomes the SE covariance function while, with $\nu = \frac{1}{2}$, it simplifies to the Absolute Exponential (AE) kernel (i.e. the covariance of a Ornstein-Uhlenbeck process):

$$k_r = A \exp\left(-\frac{r}{L}\right). \quad (2)$$

Finally, another interesting and frequently used stationary kernel is the Rational Quadratic (RQ) covariance function (Rasmussen & Williams 2006):

$$k_r = A \left[1 + \left(\frac{r^2}{2\alpha L^2}\right)^{-\alpha}\right], \quad (3)$$

with α strictly positive. This kernel can be seen as a scale mixture (i.e. an infinite sum) of SE covariance functions with different characteristic length-scales drawn from a **gamma** distribution. The limit of the RQ covariance for $\alpha \rightarrow +\infty$ is indeed just the SE covariance function with characteristic length-scale L .

In general, any covariance function mentioned above allows a satisfactory modeling of the datasets. However, having to deal with time series analysis requires some more care. The light curves considered in this work are characterized by a power spectral density (PSD) modeled by a power-law (PL) or a broken PL (see Sect. 4 and, e.g., Nilsson et al. 2018; Covino et al. 2019) and therefore it is important that the adopted covariance functions provide an adequate description of the data and their PSDs. As reported by Wilkins (2019), the SE kernel does not correctly describe the PSD of the data, in particular at low frequencies. On the contrary, the AE and RQ kernels provide better results. The best choice depends on the specific PSD functional form. The multiple length-scale sensitivity of the RQ kernel makes it an interesting choice for blazar light curves, i.e. characterized by a complex variability pattern, however the SE and AE kernels need a lower number of free parameters. We considered in our analyses both the AE and the RQ kernels, as discussed in Sect. 5.1.

Different families of kernels are needed to describe periodic behaviors. The simplest possibility is “the cosine” (CS) kernel:

$$k_r = A \cos(2\pi r/P), \quad (4)$$

where again $A > 0$ is the amplitude and r is the separation between data points. P is the period in the data.

A more flexible and also widely used covariance function is the “exp-sine-squared” (ESS) kernel (Rasmussen & Williams 2006):

$$k_r = A \exp \left[-\Gamma^2 \sin^2 \left(\frac{\pi r}{P} \right) \right], \quad (5)$$

where, if the additional parameter Γ is large, points separated by a period are strongly correlated, while the correlation is looser if Γ becomes small.

The ESS kernel offers a larger flexibility in modeling quasi-periodic phenomena, yet the CS kernel also allows negative covariances, a feature often present in case of periodic behaviors and characterizing the auto-correlation functions of the data considered in this study (see Section 5.2).

The product or the sum of two (or more) kernel functions is still a legitimate kernel function (Rasmussen & Williams 2006). The sum and product of covariance functions reflect two different scenarios. A sum of two kernels gives higher values when the first “or” the second operands support high correlation, while for the product this occurs when the first “and” the second operands are both giving high correlation. In the following we report results both for the sum and the product and adopt a kernel derived by the combination of the AE or RQ and the CS covariance functions.

The problem of determining the possible presence of a periodic behavior in a light-curve can thus be converted to a plain model comparison in a Bayesian framework (e.g., Kass & Raftery 1995; Trotta 2008; Ivezić et al. 2014; Andreon & Weaver 2015), i.e. fitting the data with a stationary kernel and a more complex model with a periodic component. We also did not define any prior on the mean function, in order not to bias our results assuming a given functional form. The procedure we followed consists in initially maximizing the likelihood function by a non-linear optimization algorithm (e.g. the Nelder-Mead or the L-BFGS-B algorithms, Gao & Han 2012; Byrd et al. 1995) and integrating the posterior probability density of the parameters of our models by a Markov Chain Monte Carlo (MCMC, Hogg & Foreman-Mackey 2018) based on the “affine-invariant Hamiltonian” and the “parallel-tempering ensemble” algorithms (Foreman-Mackey et al. 2013). We started the chains from small Gaussian balls centered on the best fit values. The first third of each chain (the “burn-in phase”) was discarded and we checked that a stationary distribution was reached (Sharma 2017). Model comparison could be carried out by evaluating the Bayesian Information Criterion (BIC, Schwarz 1978), which is simple to compute but requires that the posterior distribution of the parameters is essentially Gaussian, often an assumption not satisfied. We therefore carried out model compar-

ison by a full computation of the Bayes factors (Ivezić et al. 2014), typically much more demanding computationally, but not requiring any special assumption (see also Liddle 2007). We computed the Bayes factors, following Littlefair et al. (2017), by the so-called “thermodynamic integration” (Goggans & Chi 2004), which indeed offers an effective compromise between accuracy and computational complexity.

The model comparison to assess whether the introduction of a periodic term is preferred compared to stationary covariance functions is then carried out leaving the GP regression free to identify possible periods (within a given large range) that can then be evaluated analysing the posterior distribution of periods obtained after the analysis (Sect. 5).

Finally, the significance of the introduction of a periodic component in the modeling of the light curve has typically to be corrected for a trial factor, i.e. the number of independent frequencies that are “tried” (explicitly or implicitly) during the analysis. There is a large literature about this topic. The number of independent frequencies depends on the length of the time series and on the sampling. This is not typically a problem with a simple solution, but approximate estimates are often adequate for most practical purposes (e.g. Horne & Baliunas 1986; Schwarzenberg-Czerny 1998; Cumming 2004; Baluev 2008; Frescura et al. 2008; Zechmeister & Kürster 2009; Baluev 2013; Süveges 2014).

However, the computation of the Bayes factor already includes the multi-trial correction, since it is embedded in the integration on the allowed parameter space defined by the priors on the analysis (e.g., Gelman & Tuerlinckx 2000; Trotta 2007; Gelman et al. 2012). Effectively, the Bayes factor model selection takes into proper account all the information provided by the data.

Software tools and packages used throughout the present analyses are listed in Appendix B.

4. DATA

We selected two BL Lac objects based on the availability of well sampled optical light curves, *Fermi* high-energy data, and claims proposed in the recent literature for possible periodicities (Sect. 1). The sources are PG 1553+113, at a redshift $z \gtrsim 0.30$ (Landoni et al. 2014), and PKS 2155-304, at a redshift $z \sim 0.12$ (Falomo et al. 1991).

The optical data (*R*-band) are from several different telescopes and were already discussed in Sandrinelli et al. (2014, 2016a, 2018). Additional optical data covering the more recent epochs are reported in Appendix A. We refer the reader to the quoted papers for all the details about data reduction and analysis. The 100 MeV

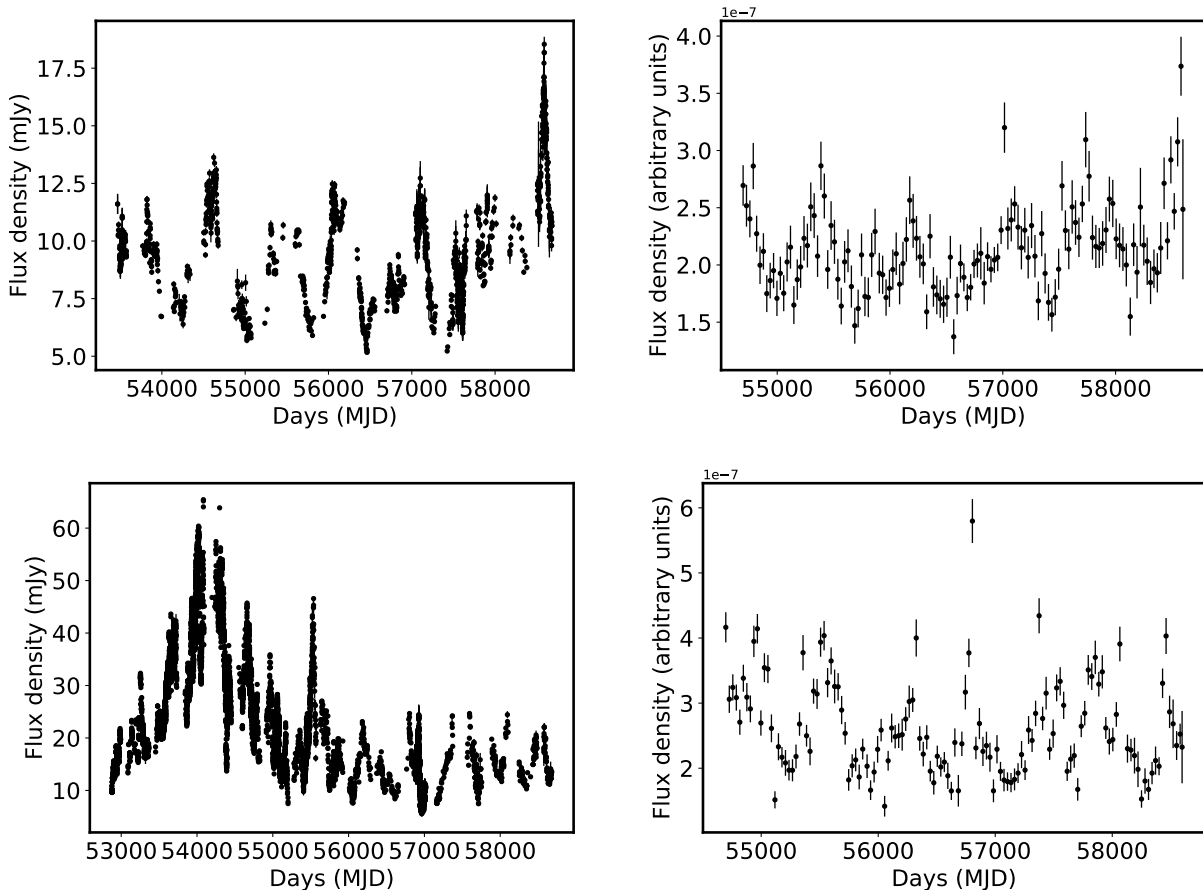


Figure 1. Optical (R -band, left column) and high-energy (100 MeV to 200 GeV, right column) light curves for the blazars considered in this study. From top to bottom, PG 1553+113 and PKS 2155-304, respectively. The optical data are shown here with the original sampling, while for the periodicity analysis they are binned at 30 days, analogously to the high-energy data.

to 200 GeV *Fermi* data have been updated with the latest observations discussed in Covino et al. (2019). Given we are mainly interested in rather long (several months) possible periodicities, optical and high-energy data are binned with a 30 day sampling. These datasets cover more than a decade of observations for all the sources considered in this work. *Fermi* data are regularly sampled, while optical data present gaps due to seasonal visibility or other problems affecting the observations (Fig. 1).

For PG 1553+113, a period of $T \sim 796$ days analyzing the *Fermi*/LAT light-curve was proposed by Ackermann et al. (2015) and the same period was reported to be consistent with data in other bands (e.g., Cutini et al. 2016; Stamerra et al. 2016). With a longer coverage the periodicity in the *Fermi* data was confirmed by Tavani et al. (2018). A consistent periodicity in the optical data, together with a confirmation at high energies, was discussed by Sandrinelli et al. (2018).

For PKS 2155-304, in the optical, a periodic component at slightly less than one year, superposed on a long-

term trend with large-amplitude variations, was proposed by Zhang et al. (2014). The same period ($T \sim 315$ days) was found by Sandrinelli et al. (2014), while a period of approximately two times the optical one ($T \sim 642$ days) was identified analyzing the *Fermi*/LAT light-curve (see also Sandrinelli et al. 2016a). Confirmation of the periodicity at high energies with a longer coverage by the *Fermi* satellite was proposed by Zhang et al. (2017a). A re-analysis of more recent data in the optical and high-energy by Sandrinelli et al. (2018) confirmed the previous findings.

These periods for both sources were also identified in the *Fermi*/LAT data by the systematic search carried out by Prokhorov & Moraghan (2017), while Covino et al. (2019) and Ait Benkhali et al. (2019) shed some doubt on the claimed significance of the proposed periodicities at high energy for these two sources (and other blazars observed by *Fermi*). Nilsson et al. (2018) also did not find any evidence for periodicity in the optical data of both sources (and other blazars well observed in the optical).

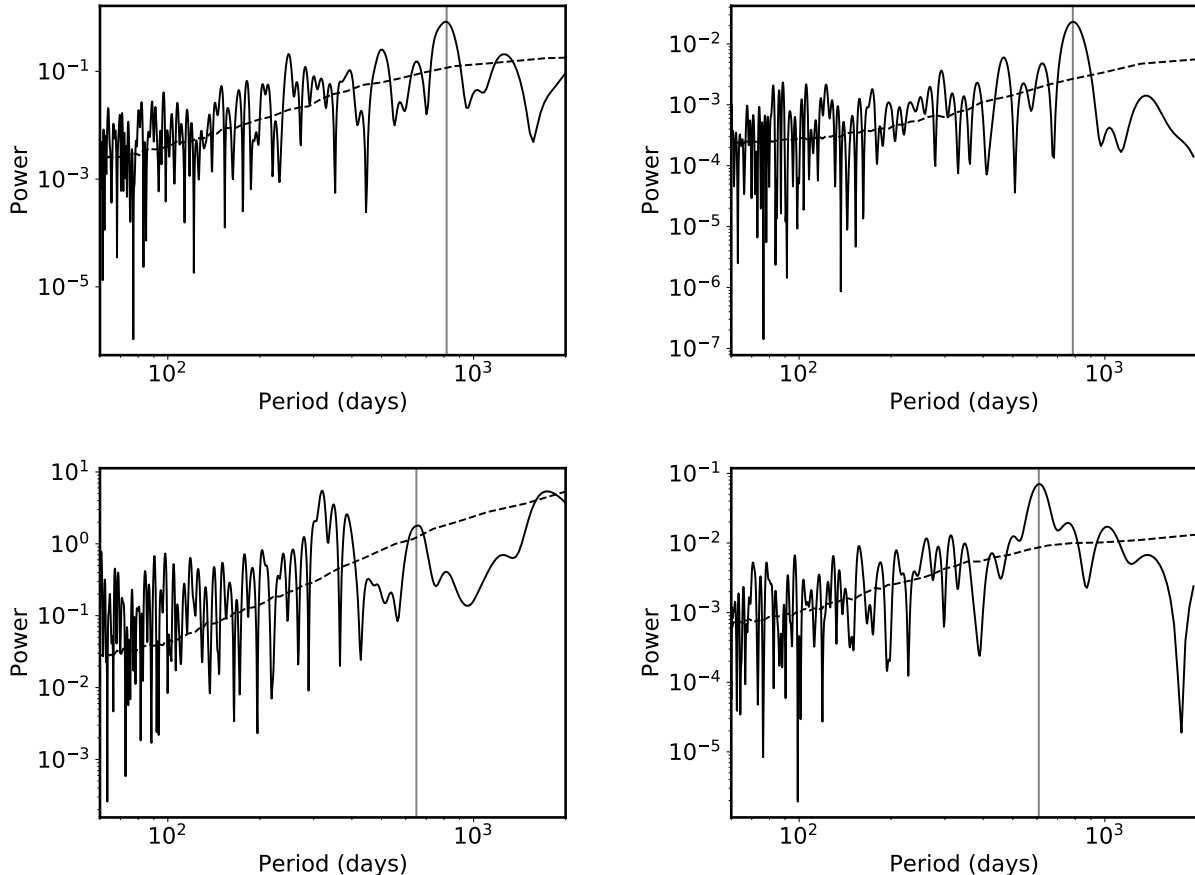


Figure 2. Optical (R -band, left column) and high-energy (100 MeV to 200 GeV, right column) Lomb-Scargle periodograms based on the light curves of the blazars considered in this study. From the top to the bottom, PG 1553+113 and PKS 2155-304, respectively. The vertical lines indicate the most prominent periods identified in the periodograms (Table 1). The dashed lines are the PSD for the best fit AE kernel (see Sect(s). 3 and 5.1).

Source	Optical period (days)	High-energy period (days)
PG 1553+113	820	790
PKS 2155-304	650	610

Table 1. Periods corresponding to the maximum power detected in the Lomb-Scargle periodograms shown in Fig. 2. The optical and high-energy light curves give consistent periods for PG 1503+113. For PKS 2155-304, in the optical, we chose to show a period similar to the high-energy one even if a single dominant feature cannot be easily identified (see Sect. 4).

5. RESULTS

The light curves for the two objects of our interest (Fig. 1) show intense variability, as it is typical for this category of sources (e.g., Lindfors et al. 2016). The high-energy and optical monitoring both cover more than a decade of observations, therefore allowing us to explore at least a few cycles for year-long periodicities.

We first checked whether our light curves are consistent with standard stationarity tests, i.e. the Augmented Dickey-Fuller unit root test (ADF) and the Kwiatkowski-Phillips-Schmidt-Shin (KPSS) test (e.g., Kwiatkowski et al. 1992; Hamilton 1994). These tests show that, to some extent, for all light curves but the high-energy data of PKS 2155-304, non-stationarity is present, as it is easy to infer even after a visual inspection (Fig. 1) due to the presence of large flares. At variance with other analysis techniques, GP regression however does not typically require one to assume stationarity of the light curves (Kovačević et al. 2019) for deriving reliable inferences.

We then carried out a period analysis by means of a generalised LS algorithm (Lomb 1976; Scargle 1982; Bretthorst 2003; VanderPlas 2018). The derived periodograms are shown in Fig. 2 and their maxima are also identified (Table 1). The PKS 2155-304 LS periodogram (Fig. 2) does not show a prominent peak, at variance with the other cases here considered. A relatively iso-

lated peak is indeed visible at ~ 650 days, close to the high-energy period. Therefore, following [Chevalier et al. \(2019\)](#), who also considered a periodicity in the optical consistent with the high-energy one, and driven by the intrinsic interest of possible synchronous periodicities in different bands, we report $P \sim 650$ days in [Fig. 2](#) and [Table 1](#).

It is also apparent that for both sources the periodograms are characterised by noise increasing toward long periods, the typical behavior when noise is correlated ([Press 1978](#); [Milotti 2002, 2007](#)). Modeling the noise as power-laws, their indices were previously evaluated in literature ([Nilsson et al. 2018](#); [Covino et al. 2019](#)) and they are approximately in the range 1 – 1.5. Given that the proposed periodicities are all close to the low-frequency tail of the derived periodograms, any evaluation of their significance has therefore to be carried out with great care (see [Sect. 2](#) and discussion in [Bhatta & Dhital 2019](#)).

5.1. Stationary kernels

For all the light curves considered in this study, we could obtain reasonable fits by GPs with any of the kernel discussed in [Sect. 3](#). This is not surprising, given the flexibility provided by GP regression, as widely discussed in literature ([Ivezić et al. 2014](#); [Littlefair et al. 2017](#); [Foreman-Mackey et al. 2017](#); [Angus et al. 2018](#)). As mentioned in [Sect. 3](#), the AE and the RQ kernels are however better suited to model our blazar light curves. Together with the considerations discussed in [Wilkins \(2019\)](#), the choice is also supported by more formal arguments, since both the RQ and the AE kernel functions are preferred over the simpler SE kernel based upon a Bayesian model comparison. In turn, the AE kernel is only moderately preferred over the RQ kernel, and for the next steps of our analysis we considered both the possibilities. In [Table 2](#) we report the computed Bayes factors. The large uninformative priors adopted in the analysis are reported in [Appendix C](#).

If the posterior probabilities of two competing models, e.g. models "0" and "1", are, respectively, p_0 and p_1 , Bayes factors can be easily converted to probabilities conditioned on the data in favor of model "1" with respect to model "0" as (e.g., [Trotta 2007](#)):

$$p = p_1/(p_0 + p_1) = BF_{0-1}/(BF_{0-1} + 1), \quad (6)$$

where $BF_{0-1} = p_0/p_1$. Therefore $BF \sim 1$ means $p \sim 50\%$, $BF \sim 10$ is slightly larger than $p \sim 90\%$ and $BF \sim 100$ gives $p \sim 99\%$.

For stationary kernels, covariance functions and PSDs are Fourier duals ([Rasmussen & Williams 2006](#)), and in [Fig. 2](#) we also show the PSD derived by the AE kernel with the best-fit parameters reported in [Appendix D](#).

Source	band	BF_{SE-RQ}	BF_{SE-AE}	BF_{RQ-AE}
PG 1553+113	HE	14 ± 2	85 ± 6	6 ± 1
	Opt	> 1000	> 1000	4 ± 1
PKS 2155-304	HE	71 ± 10	445 ± 28	6 ± 1
	Opt	> 1000	> 1000	4 ± 1

Table 2. Bayes factors for the high-energy (HE) and the optical (Opt) light-curves and the associated probabilities conditioned on the data of supporting one model (e.g. RQ or AE) over another (SE or RQ). Their 1σ credible regions are also reported. Flat uninformative or Jeffrey priors on the parameters were added to the likelihood function.

The best fit values of the parameters (also often called "hyper-parameters") of the kernel functions are not in general of straightforward interpretation. The relatively large values for the correlation length parameter L , for the AE kernel and the low values of the γ distribution parameter " α " for the RQ kernel ([Appendix D](#)) imply a correlation slowly decaying with increasing data separation ([Rasmussen & Williams 2006](#)). This is in qualitative agreement with the long-term noise correlation singled out by modeling periodograms for these sources, as e.g. in [Nilsson et al. \(2018\)](#) and [Covino et al. \(2019\)](#).

5.2. Periodic kernels

Adding a periodic component to the kernel function increases the complexity of the analysis and of course the capability of the model to reproduce the data and the associated noise. In the present work, we leave the kernel parameters essentially unconstrained with uninformative large flat or Jeffrey priors (see [Appendix C](#)). The periods, in particular, are constrained to be within a large (100-2000 day) flat range (see, e.g., [Kass & Raftery 1995](#); [Trotta 2008](#), for a discussion about prior role in Bayesian model comparison). All the adopted priors are properly normalized in order that the obtained posterior distributions are actual probability distributions (e.g., [Tak et al. 2018](#)).

We have explored all the combinations of the AE and RQ kernels with the periodic CS kernel, namely AE \times CS, RQ \times CS, AE+CS and RQ+CS, listed with increasing number of free parameters (3, 4, 4 and 5, respectively). Covariance functions including a periodic component typically yield similar results, i.e. better posterior probabilities, compared to the stationary kernel description only, as measured by the computed Bayes factors ([Table 3](#)). The preference for the description including a periodicity is partly expected basing on the results of the LS analysis and also because the two sources here considered were selected for the relevance of past peri-

odicity studies. The AE×CS combination turns out to be too simple, since the rapid decay of the covariance described by the AE kernel for separations larger than a few times the correlation length make the multiplied periodic kernel essentially ineffective. This is not the case for the RQ kernel since its greater flexibility allows it to model correlation on longer scales.

Results of the stationary vs. period kernel analysis show that there is a rather solid preference for a modeling requiring a period component for PG 1553+113, both at high energies and in the optical. On the contrary, for PKS 2155-304, the preference for a periodic component is weaker at high energy and not supported by the data in the optical.

In Fig. 3 a random selection of possible solutions, with the RQ×CS kernel, extracted for the posterior distribution of the parameters is shown superposed to the original light curves.

Even if the addition of a kernel with a periodic component is favoured by the data, it is still worth checking the obtained solutions in order to reach a better insight about the meaning of the GP regression results. To this aim, in Fig. 4, we plot the auto-correlation functions (ACF) and the best-fit based on the RQ×CS kernel function. It is clear that for PG 1553+113 and for the high-energy data of PKS 2155-304 the periodic kernel shows correlation peaks at the derived periods and the adopted covariance function correctly describe the ACF computed on the real data. Clearly, reality is richer than our models and peaks in the ACF are never repeating identically, while our models do. However, the average amplitude of the oscillations characterizing the ACFs for PG 1553+113 is larger than that for PKS 2155-304, suggesting the main reason for the lower Bayes factor obtained for the latter source. The case of the optical data of PKS 2155-304 looks different, with no evidence for an actual periodicity in the data.

A different procedure for evaluating the importance of the addition of a periodic component in the analysis is possible when covariance functions obtained by the sum of a stationary and a periodic kernel are applied (in the present study AE+CS or RQ+CS). An estimate of the role of the periodic component can be derived by the analysis of the variance associated to the latter component with respect to the former (the A_{AE} , A_{RQ} and A_{CS} parameters in Appendix D), and the marginalized posterior distribution of the variance associated to the periodic kernel. First of all, from the various fit results reported in Appendix D, we see that for the high energy data of PG 1553+113 the variance associated to the CS kernel is only slightly lower than the one associated to AE or RQ kernels, while for the optical data the periodic

kernel describes only a minor fraction of the variance associated to the stationary kernel. In general, however, the model with the RQ kernel provides more constrained parameters although, for PKS 2155-304, the variance associated to the CS kernel is always badly defined. The variance associated to the CS kernel for PG 1553+113 is greater than zero with high confidence (better than 99.97% level) at high energies and at a lower yet high level (98%) in the optical. For PKS 2155-304, the null hypothesis of zero variance associated to the periodic kernel cannot be ruled out even at a much lower confidence level.

Finally, we show the marginalized posterior distribution for the periods (Fig. 5) for the RQ+CS covariance function. This also allows us to investigate on the capabilities of a composite periodic kernel function to identify periodicities. The main peaks identified by the LS analysis (Fig. 2) are well visible, and the adopted periodicities in the analysis are confirmed. No other periods are singled out, and the distributions are clearly single-peaked with most of the posterior probabilities lying around the identified periods. Again, PKS 2155-304 in the optical is an exception, and no period stands out for this source, although minor peaks can easily be singled out.

5.3. Comparison with past results

We have selected high energy and optical data for two blazar sources with several different claims of possible QPO in literature (see Sect. 4). Summarizing, in our work we find a rather solid evidence supporting the presence of a ~ 2.2 years QPO for PG 1553+113, while for PKS 2155-304 the evidence is weaker and still inconclusive at high energies, or there is no evidence at all in the optical. The QPO in PG 1553+113 was first reported by Ackermann et al. (2015) and later confirmed by Tavani et al. (2018), while Covino et al. (2019) and Ait Benkhali et al. (2019) did not find evidence for it. For PKS 2155-304, a year-long period in the optical was suggested by Zhang et al. (2014) and a hint for a periodicity at high energy, approximately two times longer than the optical one, was suggested by Sandrinelli et al. (2016a). No periodicities in the optical for both sources emerged from the analyses by Nilsson et al. (2018).

It is therefore of interest to see the reasons for these partially (possibly apparently) contradictory results. In general, reporting a possible periodicity always depends on the comparison between a null hypothesis, i.e. the light curve is pure noise, and an hypothesis implying a periodic behavior. Independently of the specific analysis technique applied, any inference is driven by the capability to correctly interpret and model the noise of the data

Source	band	$\text{BF}_{AE-(AE \times CS)}$	$\text{BF}_{RQ-(RQ \times CS)}$	$\text{BF}_{AE-(AE+CS)}$	$\text{BF}_{RQ-(RQ+CS)}$
PG 1553+113	HE	2.0 ± 0.2	202 ± 40	223 ± 53	1709 ± 410
	Opt	7.2 ± 0.7	261 ± 51	115 ± 35	866 ± 222
PKS 2155-304	HE	1.0 ± 0.1	50 ± 11	5 ± 1	27 ± 12
	Opt	$\ll 1$	$\ll 1$	1.3 ± 0.2	1.0 ± 0.2

Table 3. Bayes factors for the high-energy (HE) and the optical (Opt) light-curves for the various combinations of stationary and period kernels considered in this study. The 1σ credible regions for the computed Bayes factors are also reported. Flat uninformative or Jeffrey priors on the parameters were added to the likelihood function.

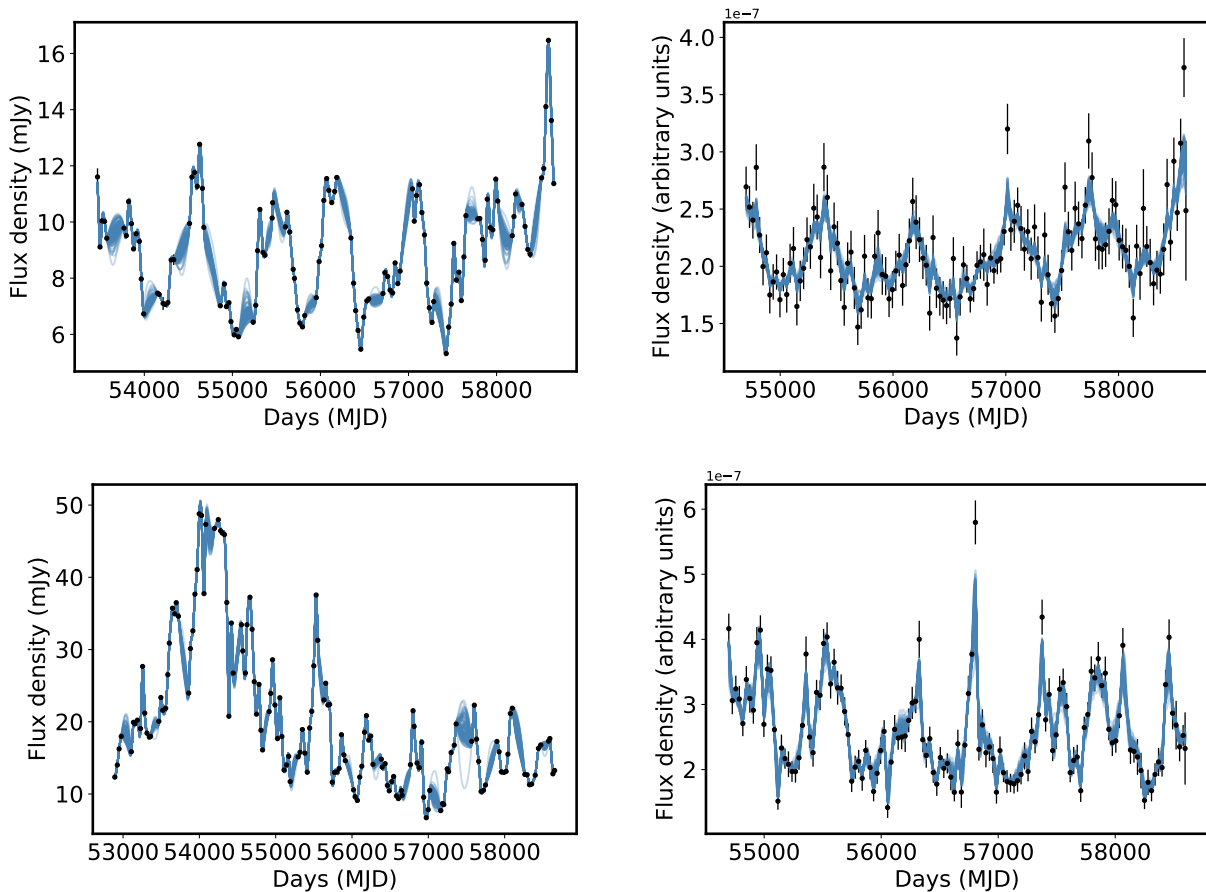


Figure 3. Fit to the light-curve based on a GP regression with a $RQ \times CS$

periodic kernel. Superposed to the light-curve a sample of 100 random set of parameters drawn for the posterior distribution is plot. Optical data (R -band, left column) and high-energy data (100 MeV to 200 GeV, right column). From the top to the bottom, PG 1553+113 and PKS 2155-304, respectively. The optical data are binned with 30 day sampling analogously to the high-energy data.

under analysis and by the capability to identify periodic behaviors. These are not trivial tasks and often remain inadequately discussed. The noise is typically modeled, implicitly or explicitly, as PLs or Broken PLs. Then, an excess power at a given frequency is compared to the prediction of the pure noise model. The power can be measured by two general sets of techniques: parametric and non-parametric. The first class includes the Fourier transform (as in Covino et al. 2019) or the popular LS

algorithm (as in Nilsson et al. 2018). These parametric techniques require to model a light curve by a harmonic decomposition, which can be ineffective in identifying even real periods in case of very noisy data and covering only a few cycles of the searched for periodicity (see also discussion in Bhatta & Dhital 2019), as it is the case of the data here considered. On the other hand, non-parametric techniques (as in Ackermann et al. 2015; Tavani et al. 2018, and for our GP analysis) do not require

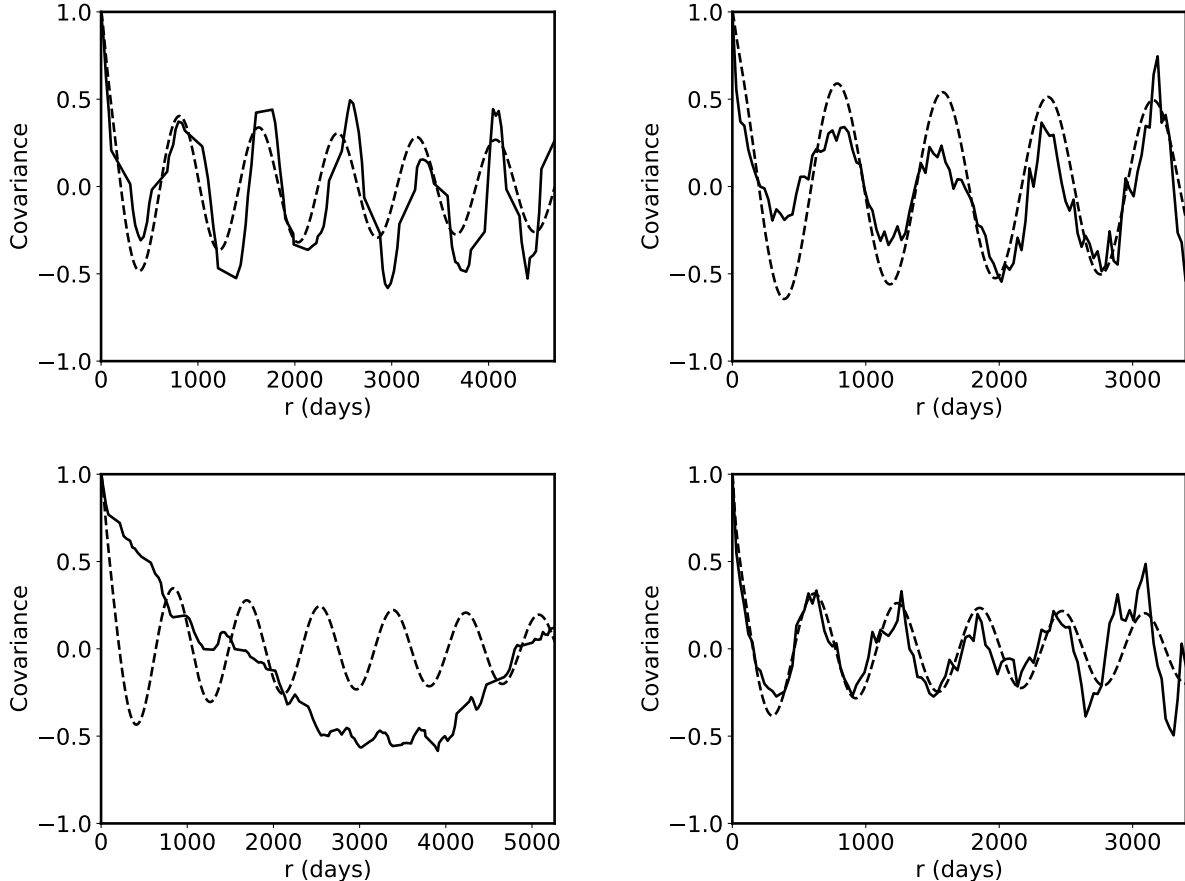


Figure 4. Plot of the best-fit RQ×CS kernel functions together with the ACF computed from the data. The quantity in abscissa, $r = (t_i - t_j)$, is the separation between data points. Optical data (*R*-band, left column) and high-energy data (100 MeV to 200 GeV, right column). From the top to the bottom, PG 1553+113 and PKS 2155-304, respectively. Dashed line for the best-fit kernel and solid line for the ACF.

one to describe the data with a given functional form and might be better suited to extract hidden periodic signals in very noisy data. A full discussion of the pros and cons of parametric and non parametric time-series analysis techniques is certainly beyond the goal of the present study. Yet, we think it is plausible that some of the different claims we mentioned are simply due to difference in the data analysis emphasized by the short coverage, in terms of number of cycles, of the available data.

6. CONCLUSIONS

In this work we addressed the problem of assessing the significance of periodicities proposed in the literature for two of the most studied blazars: PG 1553+114 and PKS 2155-304. We made use of high-energy data, from the *Fermi*/LAT instrument, and optical data collected by several telescopes. These data have partly already been analyzed in previous papers (see Sect. 4). The whole topic of blazar year-long possible periodicities is widely discussed in the literature with several pa-

pers reporting even contradicting results (see e.g. [Rieger 2019](#), for a recent discussion). Our approach is based on GP regression that, in spite of being computationally relatively demanding, offers also several advantages. The analysis does not need to be carried out in the frequency space, with all the possible problems induced by irregular sampling, gaps, etc. The inference relies on a Bayesian model comparison between two possible hypotheses: one only able to describe the correlated noise affecting blazar light curves, and another with in addition a periodic component left free to vary in the range of interest. No assumption about the form of the possible periodic variation was included in the analysis although, in presence of physically motivated scenarios, this could be done.

Our results, summarized in Tables 2 and 3, show that the addition of a periodic component always improve the description of the data, in substantial agreement with the various results in literature. For PG 1553+113 the improvement seems to be relatively solid both at high

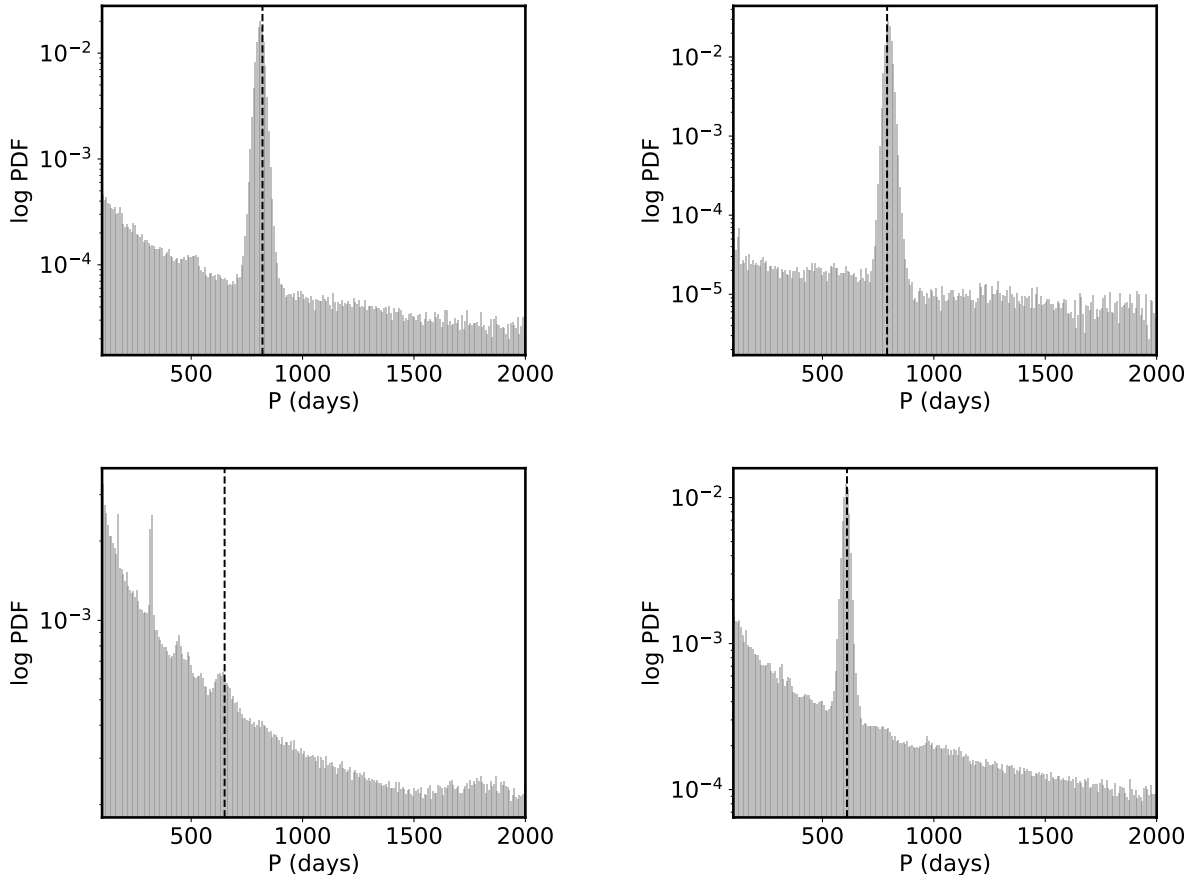


Figure 5. Marginalized posterior probability density functions for the periods singled out with the RQ+CS covariance function (results with other kernel functions are very similar). The PDF are derived by a GP regression and a flat prior from 100 to 2000 days for the optical data (*R*-band, left column) and high-energy data (100 MeV to 200 GeV, right column). From the top to the bottom, PG 1553+113 and PKS 2155-304, respectively. The vertical lines indicate the periods identified by the LS analysis (Fig. 2).

energies and in the optical, while for PKS 2155-305 the situation is still inconclusive at high energies and no periodicity seems to be present in the optical.

This is anyway at present mainly an exploratory study. Many aspects of a GP-based analysis need to be more deeply evaluated in future works. One of the most critical topic is about the choice of the covariance functions (Wilkins 2019) or the criteria for selecting the best among different possible combinations (e.g., Duveaud et al. 2013). The problem does not have in general a simple solution. Time series analyses require a modeling of the light curves and of their PSDs. We have here limited our study to the most commonly used kernel functions for GP analysis (Rasmussen & Williams 2006), but the subject is receiving increasing attention in the literature (e.g., Wilson & Prescott Adams 2013; Durrande et al. 2016; Foreman-Mackey et al. 2017; Tobar 2018).

Another interesting topic is related to the possibility to run a GP regression with multi-dimensional input data, therefore providing a natural environment to study time series available in multiple bands. The analysis can be carried out with different kernel functions in different bands, if needed, and adding a periodic kernel with the same periods for all the input data. This will allow us to optimally use all available information for statistical inference.

ACKNOWLEDGMENTS

We thank an anonymous referee for her/his rich and inspiring report. SC is grateful to dr. Luigi Stella and dr. Stefano Andreon for very profitable discussions, and to dr. Ben Granett for having carefully read the manuscript. We acknowledge partial funding from Agenzia Spaziale Italiana-Istituto Nazionale di Astrofisica grant I/004/11/3.

APPENDIX

A. OPTICAL DATA

The optical data for PG 1553+113 and PKS 2155-304 analysed in this work were partly published in Sandrinelli et al. (2014, 2016a, 2018). Here we report data obtained after the publication to the present epoch. We refer to the quoted publications for all the details about data reduction and analysis.

Tables 4 and 5, contain data for PG 1553+113 and PKS 2155-304, respectively. For both tables, Column 1 lists the MJD of the observation, Column 2 gives the R_c magnitude and Column 3 its 1σ error.

We refer the reader to the reported references for anything related to data reduction, analysis and calibration.

B. SOFTWARE PACKAGES

We have developed software tools and used third-party libraries all developed with the python language (van Rossum 1995) (v. 3.7)¹ with the usual set of scientific libraries (numpy (Oliphant 2006–) (v. 1.15.4)² and scipy (Jones et al. 2001–) (1.10)³. The ADF and KPSS stationarity tests are coded in the statsmodels library (v. 0.9.0)⁴. The generalised LS algorithm we applied is part of the astropy (v. 3.1.2)⁵ suite (Astropy Collaboration et al. 2013, 2018). ACF are computed by numpy tools. Non-linear optimization algorithms and numerical integration tools are provided by the minimize and integrate subpackages of scipy library. MCMC algorithms are provided by the emcee⁶ (v. 2.2.1) library (Foreman-Mackey et al. 2013). GP analysis is carried out by the george package (v. 0.3.1)⁷ (Ambikasaran et al. 2014). Plots are produced within the matplotlib (Hunter 2007) (v. 3.0.2)⁸ framework. Multidimensional projection plots were obtained with the corner (Foreman-Mackey 2016) (v. 2.0.2)⁹ library.

C. PRIORS IMPOSED TO THE ANALYSIS

Throughout this paper we have always adopted larger uninformative or Jeffrey priors (Table 6).

D. BEST FIT HYPER-PARAMETERS

We report here the best fit hyper-parameters obtained fitting our data with the SE kernel (Table 7), AE kernel (Table 8), the RQ kernel (Table 9), the AE×CS kernel (Table 10), the RQ×CS kernel (Table 11), the AE+CS kernel (Table 12) and the RQ+CS kernel (Table 13). For our analyses, we have multiplied the high energy and the optical data by factors 10^7 and 10^3 , respectively, for better numerical optimization. This has of course no effect on the reported results.

REFERENCES

- Ackermann, M., Ajello, M., Albert, A., et al. 2015, ApJL, 813, L41, doi: [10.1088/2041-8205/813/2/L41](https://doi.org/10.1088/2041-8205/813/2/L41)
- Ait Benkhali, F., Hofmann, W., Rieger, F. M., & Chakraborty, N. 2019, arXiv e-prints. <https://arxiv.org/abs/1901.10246>
- ¹ <http://www.python.org>
- ² <http://www.numpy.org>
- ³ <https://www.scipy.org>
- ⁴ <https://www.statsmodels.org/stable/index.html>
- ⁵ <http://www.astropy.org>
- ⁶ <http://dfm.io/emcee/current/>
- ⁷ <https://george.readthedocs.io/en/latest/>
- ⁸ <https://www.matplotlib.org>
- ⁹ <https://corner.readthedocs.io/en/latest/>
- Ambikasaran, S., Foreman-Mackey, D., Greengard, L., Hogg, D. W., & O’Neil, M. 2014
- Andreon, S., & Weaver, B. 2015, Bayesian Methods for the Physical Sciences. Learning from Examples in Astronomy and Physics., Vol. 4, doi: [10.1007/978-3-319-15287-5](https://doi.org/10.1007/978-3-319-15287-5)
- Angus, R., Morton, T., Aigrain, S., Foreman-Mackey, D., & Rajpaul, V. 2018, MNRAS, 474, 2094, doi: [10.1093/mnras/stx2109](https://doi.org/10.1093/mnras/stx2109)
- Astropy Collaboration, Robitaille, T. P., Tollerud, E. J., et al. 2013, A&A, 558, A33, doi: [10.1051/0004-6361/201322068](https://doi.org/10.1051/0004-6361/201322068)
- Astropy Collaboration, Price-Whelan, A. M., Sipőcz, B. M., et al. 2018, AJ, 156, 123, doi: [10.3847/1538-3881/aabc4f](https://doi.org/10.3847/1538-3881/aabc4f)
- Baluev, R. V. 2008, MNRAS, 385, 1279, doi: [10.1111/j.1365-2966.2008.12689.x](https://doi.org/10.1111/j.1365-2966.2008.12689.x)
- . 2013, MNRAS, 436, 807, doi: [10.1093/mnras/stt1617](https://doi.org/10.1093/mnras/stt1617)

Table 4. Optical data for PG 1553+113. Column 1 lists the MJD of the observation, Column 2 gives the R_c magnitude and Column 3 its 1σ error.

MJD	Magnitudes	1σ error
(days)	(R_c band)	
53468.40516	13.57	0.03
53495.11636	13.76	0.03
53499.10951	13.88	0.01
53501.12239	13.88	0.01
53503.10500	13.82	0.01
53506.13048	13.80	0.01
53511.17848	13.81	0.01
53518.05972	13.75	0.01
53523.03968	13.68	0.02
53526.03937	13.74	0.02
53528.03765	13.81	0.03
53538.13407	13.76	0.00
53556.10483	13.71	0.00
53573.03119	13.78	0.01
53970.04372	14.00	0.01
53995.98658	14.16	0.01
54218.26792	14.14	0.05
54234.33117	14.09	0.05
54255.12331	14.22	0.03
54331.02096	13.88	0.03
54574.25162	13.59	0.05
54588.38112	13.63	0.10
54906.38731	13.94	0.07
54921.35537	14.09	0.03
54935.38222	14.13	0.06
54950.31922	14.08	0.03
54966.27467	14.04	0.03
54982.33886	14.23	0.03
55005.27961	13.95	0.05
55028.21905	14.31	0.03
55982.37299	13.97	0.07
56011.21562	13.89	0.02
56013.24880	13.87	0.02
56016.39511	13.79	0.02
56019.32278	13.79	0.01
56021.33930	13.76	0.01
56026.22237	13.82	0.03
56029.23440	13.83	0.01
56034.21658	13.76	0.02
56036.34757	13.63	0.02
56042.22173	13.63	0.02
56047.22496	13.59	0.03
56062.35472	13.53	0.03
56065.18069	13.66	0.02
56067.36846	13.68	0.02

Table 5. Optical data for PKS 2155-304. Column 1 lists the MJD of the observation, Column 2 gives the R_c magnitude and Column 3 its 1σ error.

MJD	Magnitude	1σ error
(days)	(R_c band)	
55516.04326	12.36	0.04
55518.11836	12.51	0.05
55521.02647	12.30	0.05
55523.04867	12.20	0.03
55525.14933	12.26	0.04
55531.10888	12.41	0.04
55533.13191	12.23	0.04
55536.13616	12.11	0.04
55538.11141	12.22	0.04
55540.08721	12.44	0.04
55542.08486	12.41	0.04
55544.06030	12.38	0.04
55547.10680	12.51	0.05
55552.04550	12.59	0.05
55559.08028	12.77	0.04
55562.06174	12.70	0.04
55565.04775	12.82	0.04
55567.06705	13.02	0.03
55571.05565	12.99	0.04

Hyper-parameter	prior
$\ln A$	<i>Uniform</i> [-20, 20]
$\ln L$	<i>Uniform</i> [-20, 20]
$\ln \alpha$	<i>Uniform</i> [-10, 10]
P	<i>Uniform</i> [100, 2000]

Table 6. Prior information adopted for analyses described in Sect. 5. P_0 is the period singled out by the LS analysis. All the priors are properly normalized for the computation of the Bayes factors.

Source	band	$\ln A$	$\ln L$
PG 1553+113	HE	$-2.46^{+0.29}_{-0.26}$	$4.44^{+0.25}_{-0.39}$
	Opt	$1.17^{+0.14}_{-0.14}$	$3.42^{+0.04}_{-0.04}$
PKS 2155-304	HE	$-0.85^{+0.15}_{-0.14}$	$4.31^{+0.07}_{-0.07}$
	Opt	$4.36^{+0.13}_{-0.12}$	$3.46^{+0.03}_{-0.03}$

Table 7. 1σ credible regions and the the maximum a posterior estimator for the hyper-parameters derived by the analysis adopting the SE kernel for the high-energy (HE) and the optical (Opt) light-curves. Flat uninformative or Jeffrey priors on the parameters were added to the likelihood function.

Source	band	$\ln A$	$\ln L$
PG 1553+113	HE	$-2.14^{+0.51}_{-0.32}$	$5.24^{+0.65}_{-0.43}$
	Opt	$1.41^{+0.32}_{-0.24}$	$5.26^{+0.36}_{-0.27}$
PKS 2155-304	HE	$-0.73^{+0.22}_{-0.19}$	$4.31^{+0.28}_{-0.24}$
	Opt	$4.68^{+0.42}_{-0.29}$	$5.82^{+0.44}_{-0.31}$

Table 8. 1σ credible regions and the the maximum a posterior estimator for the hyper-parameters derived by the analysis adopting the AE kernel for the high-energy (HE) and the optical (Opt) light-curves. Flat uninformative or Jeffrey priors on the parameters were added to the likelihood function.

Source	band	$\ln A$	$\ln \alpha$	$\ln L$
PG 1553+113	HE	$-1.99^{+1.41}_{-0.47}$	$-1.45^{+1.36}_{-1.97}$	$4.11^{+0.64}_{-0.41}$
	Opt	$1.83^{+1.45}_{-0.48}$	$-1.85^{+0.85}_{-1.78}$	$3.97^{+0.70}_{-0.25}$
PKS 2155-304	HE	$-0.63^{+0.72}_{-0.24}$	$-1.00^{+0.75}_{-1.41}$	$3.28^{+0.25}_{-0.20}$
	Opt	$6.00^{+1.89}_{-1.04}$	$-3.92^{+1.19}_{-1.95}$	$4.53^{+0.94}_{-0.51}$

Table 9. 1σ credible regions and the the maximum a posterior estimator for the hyper-parameters derived by the analysis adopting the RQ kernel for the high-energy (HE) and the optical (Opt) light-curves. Flat uninformative or Jeffrey priors on the parameters were added to the likelihood function.

Source	band	$\ln A$	$\ln L$	$\ln P$
PG 1553+113	HE	$-2.18^{+0.44}_{-0.33}$	$5.58^{+0.67}_{-0.52}$	$6.95^{+0.38}_{-0.28}$
	Opt	$1.42^{+0.28}_{-0.23}$	$5.43^{+0.32}_{-0.28}$	$6.92^{+0.35}_{-0.25}$
PKS 2155-304	HE	$-0.74^{+0.22}_{-0.19}$	$4.39^{+0.30}_{-0.27}$	$6.89^{+0.47}_{-0.47}$
	Opt	$4.55^{+0.31}_{-0.24}$	$5.68^{+0.33}_{-0.27}$	$7.51^{+0.07}_{-0.13}$

Table 10. 1σ credible regions and the the maximum a posterior estimator for the hyper-parameters derived by the analysis adopting the AE \times CS kernel for the high-energy (HE) and the optical (Opt) light-curves. Flat uninformative or Jeffrey priors on the parameters were added to the likelihood function.

Source	band	$\ln A$	$\ln \alpha$	$\ln L$	$\ln P$
PG 1553+113	HE	$-1.93^{+1.03}_{-0.52}$	$-2.79^{+0.93}_{-1.34}$	$3.58^{+0.69}_{-0.94}$	$6.67^{+0.04}_{-0.03}$
	Opt	$1.58^{+0.79}_{-0.38}$	$-2.13^{+0.63}_{-1.05}$	$3.85^{+0.37}_{-0.21}$	$6.71^{+0.06}_{-0.04}$
PKS 2155-304	HE	$-0.58^{+0.71}_{-0.31}$	$-2.05^{+0.75}_{-1.20}$	$2.90^{+0.39}_{-0.70}$	$6.44^{+0.13}_{-0.06}$
	Opt	$5.28^{+1.15}_{-0.64}$	$-3.02^{+0.84}_{-1.27}$	$4.20^{+0.57}_{-0.32}$	$7.55^{+0.04}_{-0.07}$

Table 11. 1σ credible regions and the the maximum a posterior estimator for the hyper-parameters derived by the analysis adopting the RQ \times CS kernel for the high-energy (HE) and the optical (Opt) light-curves. Flat uninformative or Jeffrey priors on the parameters were added to the likelihood function.

Source	band	$\ln A_{AE}$	$\ln L$	$\ln A_{CS}$	$\ln P$
PG 1553+113	HE	$-2.76^{+0.52}_{-0.32}$	$4.81^{+0.64}_{-0.48}$	$-3.20^{+1.31}_{-2.11}$	$6.68^{+0.03}_{-0.03}$
	Opt	$1.17^{+0.40}_{-0.32}$	$5.05^{+0.42}_{-0.34}$	$-0.66^{+1.91}_{-12.0}$	$6.69^{+0.05}_{-0.86}$
PKS 2155-304	HE	$-0.97^{+0.25}_{-0.20}$	$4.02^{+0.34}_{-0.29}$	$-11.6^{+5.9}_{-5.7}$	$6.41^{+0.03}_{-0.04}$
	Opt	$4.70^{+0.47}_{-0.31}$	$5.84^{+0.49}_{-0.33}$	$-8.84^{+7.46}_{-7.54}$	$6.09^{+1.04}_{-0.98}$

Table 12. 1σ credible regions and the the maximum a posterior estimator for the hyper-parameters derived by the analysis adopting the AE+CS kernel for the high-energy (HE) and the optical (Opt) light-curves. Flat uninformative or Jeffrey priors on the parameters were added to the likelihood function.

Source	band	$\ln A_{RQ}$	$\ln \alpha$	$\ln L$	$\ln A_{CS}$	$\ln P$
PG 1553+113	HE	$-2.37^{+1.83}_{-0.62}$	$-2.36^{+1.59}_{-2.41}$	$3.36^{+0.75}_{-1.15}$	$-2.89^{+1.39}_{-1.08}$	$6.68^{+0.02}_{-0.02}$
	Opt	$1.27^{+1.26}_{-0.42}$	$-1.48^{+0.81}_{-1.70}$	$3.69^{+0.59}_{-0.21}$	$0.26^{+1.44}_{-1.95}$	$6.70^{+0.02}_{-0.03}$
PKS 2155-304	HE	$-0.73^{+0.87}_{-0.33}$	$-0.98^{+1.05}_{-1.70}$	$3.19^{+0.30}_{-0.29}$	$-4.52^{+3.00}_{-10.5}$	$6.40^{+0.35}_{-0.84}$
	Opt	$6.11^{+2.08}_{-1.14}$	$-4.04^{+1.29}_{-2.13}$	$4.58^{+1.03}_{-0.56}$	$-8.93^{+7.58}_{-7.53}$	$6.15^{+1.03}_{-1.01}$

Table 13. 1σ credible regions and the maximum a posterior estimator for the hyper-parameters derived by the analysis adopting the RQ+CS kernel for the high-energy (HE) and the optical (Opt) light-curves. Flat uninformative or Jeffrey priors on the parameters were added to the likelihood function.

- Barret, D., & Vaughan, S. 2012, *ApJ*, 746, 131, doi: [10.1088/0004-637X/746/2/131](https://doi.org/10.1088/0004-637X/746/2/131)
- Bhatta, G. 2019, *MNRAS*, 487, 3990, doi: [10.1093/mnras/stz1482](https://doi.org/10.1093/mnras/stz1482)
- Bhatta, G., & Dhital, N. 2019, arXiv e-prints, arXiv:1911.08198. <https://arxiv.org/abs/1911.08198>
- Bretthorst, G. L. 2003, Frequency estimation and generalized Lomb-Scargle periodograms, ed. E. D. Feigelson & G. J. Babu, 309–329
- Brewer, B. J., & Stello, D. 2009, *MNRAS*, 395, 2226, doi: [10.1111/j.1365-2966.2009.14679.x](https://doi.org/10.1111/j.1365-2966.2009.14679.x)
- Byrd, R., Lu, P., Nosedal, J., & Zhu, C. 1995, *SIAM Journal of Scientific Computing*, 16, 1190, doi: [10.1137/0916069](https://doi.org/10.1137/0916069)
- Camenzind, M., & Krockenberger, M. 1992, *A&A*, 255, 59
- Caproni, A., Abraham, Z., Motter, J. C., & Monteiro, H. 2017, *ApJL*, 851, L39, doi: [10.3847/2041-8213/aa9fea](https://doi.org/10.3847/2041-8213/aa9fea)
- Cavaliere, A., Tavani, M., Munar-Adrover, P., & Argan, A. 2019, *ApJ*, 875, L22, doi: [10.3847/2041-8213/ab0e88](https://doi.org/10.3847/2041-8213/ab0e88)
- Cavaliere, A., Tavani, M., & Vittorini, V. 2017, *ApJ*, 836, 220, doi: [10.3847/1538-4357/836/2/220](https://doi.org/10.3847/1538-4357/836/2/220)
- Chevalier, J., Sanchez, D. A., Serpico, P. D., Lenain, J.-P., & Maurin, G. 2019, *MNRAS*, 484, 749, doi: [10.1093/mnras/stz027](https://doi.org/10.1093/mnras/stz027)
- Chua, A. J. K., Korsakova, N., Moore, C. J., Gair, J. R., & Babak, S. 2019, arXiv e-prints, arXiv:1912.11543. <https://arxiv.org/abs/1912.11543>
- Covino, S., Sandrinelli, A., & Treves, A. 2017, in *IAU Symposium*, Vol. 324, *New Frontiers in Black Hole Astrophysics*, ed. A. Gomboc, 180–183, doi: [10.1017/S174392131700237X](https://doi.org/10.1017/S174392131700237X)
- Covino, S., Sandrinelli, A., & Treves, A. 2019, *MNRAS*, 482, 1270, doi: [10.1093/mnras/sty2720](https://doi.org/10.1093/mnras/sty2720)
- Cumming, A. 2004, *MNRAS*, 354, 1165, doi: [10.1111/j.1365-2966.2004.08275.x](https://doi.org/10.1111/j.1365-2966.2004.08275.x)
- Cutini, S., Ciprini, S., Stamerra, A., Thompson, D. J., & Perri, M. 2016, in *Active Galactic Nuclei 12: A Multi-Messenger Perspective (AGN12)*, 58, doi: [10.5281/zenodo.163819](https://doi.org/10.5281/zenodo.163819)
- Doğan, S., Nixon, C., King, A., & Price, D. J. 2015, *MNRAS*, 449, 1251, doi: [10.1093/mnras/stv347](https://doi.org/10.1093/mnras/stv347)
- Durrande, N., Hensman, J., Rattray, M., & D. Lawrence, N. 2016, *PeerJ Computer Science*, 2, e50, doi: [10.7717/peerj-cs.50](https://doi.org/10.7717/peerj-cs.50)
- Duvenaud, D., Lloyd, J. R., Grosse, R., Tenenbaum, J. B., & Ghahramani, Z. 2013, arXiv e-prints, arXiv:1302.4922. <https://arxiv.org/abs/1302.4922>
- Elorrieta, F., Eyheramendy, S., & Palma, W. 2019, *A&A*, 627, A120, doi: [10.1051/0004-6361/201935560](https://doi.org/10.1051/0004-6361/201935560)
- Falomo, R., Giraud, E., Maraschi, L., et al. 1991, *ApJL*, 380, L67, doi: [10.1086/186175](https://doi.org/10.1086/186175)
- Feigelson, E. D., Babu, G. J., & Caceres, G. A. 2018, *Frontiers in Physics*, 6, 80, doi: [10.3389/fphy.2018.00080](https://doi.org/10.3389/fphy.2018.00080)
- Foreman-Mackey, D. 2016, *The Journal of Open Source Software*, 24, doi: [10.21105/joss.00024](https://doi.org/10.21105/joss.00024)
- Foreman-Mackey, D., Agol, E., Ambikasaran, S., & Angus, R. 2017, *AJ*, 154, 220, doi: [10.3847/1538-3881/aa9332](https://doi.org/10.3847/1538-3881/aa9332)
- Foreman-Mackey, D., Hogg, D. W., Lang, D., & Goodman, J. 2013, *PASP*, 125, 306, doi: [10.1086/670067](https://doi.org/10.1086/670067)
- Frescura, F. A. M., Engelbrecht, C. A., & Frank, B. S. 2008, *MNRAS*, 388, 1693, doi: [10.1111/j.1365-2966.2008.13499.x](https://doi.org/10.1111/j.1365-2966.2008.13499.x)
- Gao, F., & Han, L. 2012, *Comp. Opt. and Appl.*, 51, 259
- Gelman, A., Hill, J., & Masanao, Y. 2012, *Journal of Research on Educational Effectiveness*, 5, 189
- Gelman, A., & Tuerlinckx, F. 2000, *Computational Statistics*, 15, 373
- Goggans, P. M., & Chi, Y. 2004, in *American Institute of Physics Conference Series*, Vol. 707, *Bayesian Inference and Maximum Entropy Methods in Science and Engineering*, ed. G. J. Erickson & Y. Zhai, 59–66, doi: [10.1063/1.1751356](https://doi.org/10.1063/1.1751356)
- Graham, M. J., Djorgovski, S. G., Stern, D., et al. 2015, *MNRAS*, 453, 1562, doi: [10.1093/mnras/stv1726](https://doi.org/10.1093/mnras/stv1726)
- Guidorzi, C., Dichiara, S., & Amati, L. 2016, *A&A*, 589, A98, doi: [10.1051/0004-6361/201527642](https://doi.org/10.1051/0004-6361/201527642)
- Hamilton, J. 1994, *Time series analysis* (Princeton, NJ: Princeton Univ. Press). http://gso.gbv.de/DB=2.1/CMD?ACT=SRCHA&SRT=YOP&IKT=1016&TRM=ppn+126800421&sourceid=fwb_bibsonomy
- Hara, N. C., Boué, G., Laskar, J., & Correia, A. C. M. 2017, *MNRAS*, 464, 1220, doi: [10.1093/mnras/stw2261](https://doi.org/10.1093/mnras/stw2261)
- Haywood, R. D., Collier Cameron, A., Queloz, D., et al. 2014, *MNRAS*, 443, 2517, doi: [10.1093/mnras/stu1320](https://doi.org/10.1093/mnras/stu1320)
- Hogg, D. W., & Foreman-Mackey, D. 2018, *ApJS*, 236, 11, doi: [10.3847/1538-4365/aab76e](https://doi.org/10.3847/1538-4365/aab76e)
- Holgado, A. M., Sesana, A., Sandrinelli, A., et al. 2018, *MNRAS*, 481, L74, doi: [10.1093/mnrasl/sly158](https://doi.org/10.1093/mnrasl/sly158)
- Horne, J. H., & Baliunas, S. L. 1986, *ApJ*, 302, 757, doi: [10.1086/164037](https://doi.org/10.1086/164037)
- Huijse, P., Estévez, P. A., Förster, F., et al. 2018, *ApJS*, 236, 12, doi: [10.3847/1538-4365/aab77c](https://doi.org/10.3847/1538-4365/aab77c)
- Hunter, J. D. 2007, *Computing In Science & Engineering*, 9, 90, doi: [10.1109/MCSE.2007.55](https://doi.org/10.1109/MCSE.2007.55)
- Israel, G. L., & Stella, L. 1996, *ApJ*, 468, 369, doi: [10.1086/177697](https://doi.org/10.1086/177697)
- Ivezić, Ž., Connolly, A. J., VanderPlas, J. T., & Gray, A. 2014, *Statistics, Data Mining, and Machine Learning in Astronomy*

- Jesus, J. F., Valentim, R., Escobal, A. A., & Pereira, S. H. 2019, arXiv e-prints, arXiv:1909.00090.
<https://arxiv.org/abs/1909.00090>
- Jones, E., Oliphant, T., Peterson, P., et al. 2001–, SciPy: Open source scientific tools for Python.
<http://www.scipy.org/>
- Karamanavis, V. 2017, *Galaxies*, 5, 19,
 doi: [10.3390/galaxies5010019](https://doi.org/10.3390/galaxies5010019)
- Kass, R. E., & Raftery, A. E. 1995, *Journal of the American Statistical Association*, 90, 773.
<http://www.jstor.org/stable/2291091>
- Kelly, B. C., Bechtold, J., & Siemiginowska, A. 2009, *ApJ*, 698, 895, doi: [10.1088/0004-637X/698/1/895](https://doi.org/10.1088/0004-637X/698/1/895)
- Kelly, B. C., Becker, A. C., Sobolewska, M., Siemiginowska, A., & Uttley, P. 2014, *ApJ*, 788, 33,
 doi: [10.1088/0004-637X/788/1/33](https://doi.org/10.1088/0004-637X/788/1/33)
- Koen, C. 1990, *ApJ*, 348, 700, doi: [10.1086/168277](https://doi.org/10.1086/168277)
- . 2005, *MNRAS*, 361, 887,
 doi: [10.1111/j.1365-2966.2005.09213.x](https://doi.org/10.1111/j.1365-2966.2005.09213.x)
- Kovačević, A. B., Popović, L. Č., Simić, S., & Ilić, D. 2019, *ApJ*, 871, 32, doi: [10.3847/1538-4357/aaf731](https://doi.org/10.3847/1538-4357/aaf731)
- Kwiatkowski, D., Phillips, P., Schmidt, P., & Shin, Y. 1992, *Journal of Econometrics*, 54, 159.
<https://EconPapers.repec.org/RePEc:eee:econom:v:54:y:1992:i:1-3:p:159-178>
- Landoni, M., Falomo, R., Treves, A., & Sbarufatti, B. 2014, *A&A*, 570, A126, doi: [10.1051/0004-6361/201424232](https://doi.org/10.1051/0004-6361/201424232)
- Lehto, H. J., & Valtonen, M. J. 1996, *ApJ*, 460, 207,
 doi: [10.1086/176962](https://doi.org/10.1086/176962)
- Lenoir, G., & Crucifix, M. 2018, *Nonlinear Processes in Geophysics*, 25, 145, doi: [10.5194/npg-25-145-2018](https://doi.org/10.5194/npg-25-145-2018)
- Li, Y.-R., & Wang, J.-M. 2018, *MNRAS*, 476, L55,
 doi: [10.1093/mnrasl/sly028](https://doi.org/10.1093/mnrasl/sly028)
- Lico, R., Liu, J., Giroletti, M., et al. 2020, *A&A*, 634, A87,
 doi: [10.1051/0004-6361/201936564](https://doi.org/10.1051/0004-6361/201936564)
- Liddle, A. R. 2007, *MNRAS*, 377, L74,
 doi: [10.1111/j.1745-3933.2007.00306.x](https://doi.org/10.1111/j.1745-3933.2007.00306.x)
- Lindfors, E. J., Hovatta, T., Nilsson, K., et al. 2016, *A&A*, 593, A98, doi: [10.1051/0004-6361/201628420](https://doi.org/10.1051/0004-6361/201628420)
- Littlefair, S. P., Burningham, B., & Helling, C. 2017, *MNRAS*, 466, 4250, doi: [10.1093/mnras/stw3376](https://doi.org/10.1093/mnras/stw3376)
- Lomb, N. R. 1976, *Ap&SS*, 39, 447,
 doi: [10.1007/BF00648343](https://doi.org/10.1007/BF00648343)
- Luger, R., Agol, E., Kruse, E., et al. 2016, *AJ*, 152, 100,
 doi: [10.3847/0004-6256/152/4/100](https://doi.org/10.3847/0004-6256/152/4/100)
- Marscher, A. P. 2014, *ApJ*, 780, 87,
 doi: [10.1088/0004-637X/780/1/87](https://doi.org/10.1088/0004-637X/780/1/87)
- Milotti, E. 2002, *ArXiv Physics e-prints*
- . 2007, *PhRvE*, 75, 011120,
 doi: [10.1103/PhysRevE.75.011120](https://doi.org/10.1103/PhysRevE.75.011120)
- Nilsson, K., Lindfors, E., Takalo, L. O., et al. 2018, *A&A*, 620, A185, doi: [10.1051/0004-6361/201833621](https://doi.org/10.1051/0004-6361/201833621)
- Oliphant, T. 2006–, *NumPy: A guide to NumPy*, USA: Trelgol Publishing. <http://www.numpy.org/>
- Pereira, F., Campante, T. L., Cunha, M. S., et al. 2019, *MNRAS*, 489, 5764, doi: [10.1093/mnras/stz2405](https://doi.org/10.1093/mnras/stz2405)
- Press, W. H. 1978, *Comments on Astrophysics*, 7, 103
- Prokhorov, D. A., & Moraghan, A. 2017, *MNRAS*, 471, 3036, doi: [10.1093/mnras/stx1742](https://doi.org/10.1093/mnras/stx1742)
- Raiteri, C. M., Villata, M., Acosta-Pulido, J. A., et al. 2017, *Nature*, 552, 374, doi: [10.1038/nature24623](https://doi.org/10.1038/nature24623)
- Rajpaul, V., Aigrain, S., Osborne, M. A., Reece, S., & Roberts, S. 2015, *MNRAS*, 452, 2269,
 doi: [10.1093/mnras/stv1428](https://doi.org/10.1093/mnras/stv1428)
- Rasmussen, C. E., & Williams, C. K. I. 2006, *Gaussian Processes for Machine Learning*
- Rieger, F. 2019, *Galaxies*, 7, 28,
 doi: [10.3390/galaxies7010028](https://doi.org/10.3390/galaxies7010028)
- Roberts, S., Osborne, M., Ebden, M., et al. 2012, *Philosophical Transactions of the Royal Society of London Series A*, 371, 20110550,
 doi: [10.1098/rsta.2011.0550](https://doi.org/10.1098/rsta.2011.0550)
- Ryan, J. L., Siemiginowska, A., Sobolewska, M. A., & Grindlay, J. 2019, *ApJ*, 885, 12,
 doi: [10.3847/1538-4357/ab426a](https://doi.org/10.3847/1538-4357/ab426a)
- Sandrinelli, A., Covino, S., Dotti, M., & Treves, A. 2016a, *AJ*, 151, 54, doi: [10.3847/0004-6256/151/3/54](https://doi.org/10.3847/0004-6256/151/3/54)
- Sandrinelli, A., Covino, S., & Treves, A. 2014, *ApJL*, 793, L1, doi: [10.1088/2041-8205/793/1/L1](https://doi.org/10.1088/2041-8205/793/1/L1)
- . 2016b, *ApJ*, 820, 20, doi: [10.3847/0004-637X/820/1/20](https://doi.org/10.3847/0004-637X/820/1/20)
- Sandrinelli, A., Covino, S., Treves, A., et al. 2018, *A&A*, 615, A118, doi: [10.1051/0004-6361/201732550](https://doi.org/10.1051/0004-6361/201732550)
- . 2017, *A&A*, 600, A132,
 doi: [10.1051/0004-6361/201630288](https://doi.org/10.1051/0004-6361/201630288)
- Scargle, J. D. 1982, *ApJ*, 263, 835, doi: [10.1086/160554](https://doi.org/10.1086/160554)
- Schwarz, G. 1978, *Ann. Statist.*, 6, 461,
 doi: [10.1214/aos/1176344136](https://doi.org/10.1214/aos/1176344136)
- Schwarzenberg-Czerny, A. 1997, *ApJ*, 489, 941,
 doi: [10.1086/304832](https://doi.org/10.1086/304832)
- . 1998, *MNRAS*, 301, 831,
 doi: [10.1046/j.1365-8711.1998.02086.x](https://doi.org/10.1046/j.1365-8711.1998.02086.x)
- Sharma, S. 2017, *ARA&A*, 55, 213,
 doi: [10.1146/annurev-astro-082214-122339](https://doi.org/10.1146/annurev-astro-082214-122339)
- Sobacchi, E., Sormani, M. C., & Stamerra, A. 2017, *MNRAS*, 465, 161, doi: [10.1093/mnras/stw2684](https://doi.org/10.1093/mnras/stw2684)
- Stamerra, A., Prandini, E., Paiano, S., et al. 2016, in *Active Galactic Nuclei 12: A Multi-Messenger Perspective (AGN12)*, 64, doi: [10.5281/zenodo.163826](https://doi.org/10.5281/zenodo.163826)
- Stellingwerf, R. F. 1978, *ApJ*, 224, 953, doi: [10.1086/156444](https://doi.org/10.1086/156444)

- Sulis, S., Mary, D., & Bigot, L. 2017, *IEEE Transactions on Signal Processing*, 65, 2136, doi: [10.1109/TSP.2017.2652391](https://doi.org/10.1109/TSP.2017.2652391)
- Süveges, M. 2014, *MNRAS*, 440, 2099, doi: [10.1093/mnras/stu372](https://doi.org/10.1093/mnras/stu372)
- Süveges, M., Guy, L. P., Eyer, L., et al. 2015, *MNRAS*, 450, 2052, doi: [10.1093/mnras/stv719](https://doi.org/10.1093/mnras/stv719)
- Tak, H., Ghosh, S. K., & Ellis, J. A. 2018, *MNRAS*, 481, 277, doi: [10.1093/mnras/sty2326](https://doi.org/10.1093/mnras/sty2326)
- Takata, T., Mukuta, Y., & Mizumoto, Y. 2018, *ApJ*, 869, 178, doi: [10.3847/1538-4357/aaef31](https://doi.org/10.3847/1538-4357/aaef31)
- Tavani, M., Cavaliere, A., Munar-Adrover, P., & Argan, A. 2018, *ApJ*, 854, 11, doi: [10.3847/1538-4357/aaa3f4](https://doi.org/10.3847/1538-4357/aaa3f4)
- Tobar, F. 2018, in *Advances in Neural Information Processing Systems 31*, ed. S. Bengio, H. Wallach, H. Larochelle, K. Grauman, N. Cesa-Bianchi, & R. Garnett (Curran Associates, Inc.), 10127–10137. <http://papers.nips.cc/paper/8216-bayesian-nonparametric-spectral-estimation.pdf>
- Tobar, F., Bui, T. D., & Turner, R. E. 2015, in *Advances in Neural Information Processing Systems 28*, ed. C. Cortes, N. D. Lawrence, D. D. Lee, M. Sugiyama, & R. Garnett (Curran Associates, Inc.), 3501–3509. <http://papers.nips.cc/paper/5772-learning-stationary-time-series-using-gaussian-processes-with-nonparametric-kernels.pdf>
- Trotta, R. 2007, *MNRAS*, 378, 72, doi: [10.1111/j.1365-2966.2007.11738.x](https://doi.org/10.1111/j.1365-2966.2007.11738.x)
- . 2008, *Contemporary Physics*, 49, 71, doi: [10.1080/001075108020666753](https://doi.org/10.1080/001075108020666753)
- Urry, M. 2012, *Astronomical Review*, 7, 4, doi: [10.1080/21672857.2012.11519698](https://doi.org/10.1080/21672857.2012.11519698)
- Uttley, P., McHardy, I. M., & Papadakis, I. E. 2002, *MNRAS*, 332, 231, doi: [10.1046/j.1365-8711.2002.05298.x](https://doi.org/10.1046/j.1365-8711.2002.05298.x)
- van der Klis, M. 1989, *ARA&A*, 27, 517, doi: [10.1146/annurev.aa.27.090189.002505](https://doi.org/10.1146/annurev.aa.27.090189.002505)
- van Rossum, G. 1995, Python tutorial, Tech. Rep. CS-R9526, Centrum voor Wiskunde en Informatica (CWI), Amsterdam
- Vanderburg, A., Montet, B. T., Johnson, J. A., et al. 2015, *ApJ*, 800, 59, doi: [10.1088/0004-637X/800/1/59](https://doi.org/10.1088/0004-637X/800/1/59)
- VanderPlas, J. T. 2018, *ApJS*, 236, 16, doi: [10.3847/1538-4365/aab766](https://doi.org/10.3847/1538-4365/aab766)
- Vaughan, S. 2010, *MNRAS*, 402, 307, doi: [10.1111/j.1365-2966.2009.15868.x](https://doi.org/10.1111/j.1365-2966.2009.15868.x)
- . 2013, arXiv e-prints, arXiv:1309.6435. <https://arxiv.org/abs/1309.6435>
- Vaughan, S., Uttley, P., Markowitz, A. G., et al. 2016, *MNRAS*, 461, 3145, doi: [10.1093/mnras/stw1412](https://doi.org/10.1093/mnras/stw1412)
- Vio, R., & Andreani, P. 2018, ArXiv e-prints. <https://arxiv.org/abs/1807.01595>
- Wang, Y., Khardon, R., & Protopapas, P. 2012, *The Astrophysical Journal*, 756, 67, doi: [10.1088/0004-637x/756/1/67](https://doi.org/10.1088/0004-637x/756/1/67)
- Wilkins, D. R. 2019, *MNRAS*, 489, 1957, doi: [10.1093/mnras/stz2269](https://doi.org/10.1093/mnras/stz2269)
- Wilson, A. G., & Prescott Adams, R. 2013, arXiv e-prints, arXiv:1302.4245. <https://arxiv.org/abs/1302.4245>
- Zechmeister, M., & Kürster, M. 2009, *A&A*, 496, 577, doi: [10.1051/0004-6361:200811296](https://doi.org/10.1051/0004-6361:200811296)
- Zhang, B.-K., Zhao, X.-Y., Wang, C.-X., & Dai, B.-Z. 2014, *Research in Astronomy and Astrophysics*, 14, 933, doi: [10.1088/1674-4527/14/8/004](https://doi.org/10.1088/1674-4527/14/8/004)
- Zhang, P.-f., Yan, D.-h., Liao, N.-h., & Wang, J.-c. 2017a, *ApJ*, 835, 260, doi: [10.3847/1538-4357/835/2/260](https://doi.org/10.3847/1538-4357/835/2/260)
- Zhang, P.-f., Yan, D.-h., Liao, N.-h., et al. 2017b, *ApJ*, 842, 10, doi: [10.3847/1538-4357/aa7465](https://doi.org/10.3847/1538-4357/aa7465)
- Zhang, P.-F., Yan, D.-H., Zhou, J.-N., et al. 2017c, *ApJ*, 845, 82, doi: [10.3847/1538-4357/aa7ecdd](https://doi.org/10.3847/1538-4357/aa7ecdd)